challenged. Lower-frequency lasers are being developed for this purpose. The Fourier-transform spectrometer will also be modified as to place the low-temperature detector and the sample in separate cryostats. The temperature of the specimen can then be raised to excite free electrons for cyclotron resonance.

The cyclotron-resonance mass has also been found to change as the temperature is increased to 55 K. This will be investigated by repeating the measurements on specimens of different carrier concentration and different size.

Finally, a cyclotron-resonance mass of $0.24m_0$ for $H \perp c$ has been measured. This cyclotron-resonance anisotropy is inverse to the anisotropy measured from the Zeeman splitting where 0.34 m_0 was obtained for $H \perp c$. It will be necessary to develop a theoretical model for the shallow bound states before the splitting can be interpreted quantitatively.

We wish to thank C. W. Litton, D. C. Reynolds, and G. Landwehr for profitable discussions, and W. Dreybrodt for early participation in the cyclotron-resonance experiments. We are grateful to R. E. Newcomb, F. Tambini, E. Sudenfield, and J. Christensen for technical assistance.

*Work supported by Max Kade Foundation, on leave of absence from Physikalisches Institut der Universität Würzburg, Würzberg, Germany.

†Also Physics Department, Massachusetts Institute of Technology.

‡Work supported by the National Science Foundation.

[1]P. Wagner, Diplom-These, Universität Erlangen, Germany, 1971 (unpublished); for Hall-effect measurements and a detailed discussion see P. Wagner and R. Helbig, to be published.

[2]R. Helbig, J. Cryst. Growth 15, 25 (1972).

[3]K. J. Button and B. Lax, in *Submillimeter Waves*, (Polytechnic Press of the Polytechnic Institute of Brooklyn, Brooklyn, N. Y., 1970); K. J. Button, in *Optical Properties of Solids*, edited by E. D. Haidemenakis (Gordon and Breach, New York, 1970), pp. 253–279, and Laser Focus 7, 29 (1971).

[4]W. S. Baer, Phys. Rev. 154, 785 (1967).

[5]R. L. Weiher, Phys. Rev. 152, 736 (1966).

[6]E. Mollwo and R. Till, Z. Phys. 216, 315 (1968).

Electronic Structure and Kinetics of the Oxidation of Ba and Sr†

Kenneth A. Kress* and Gerald J. Lapeyre
Montana State University, Bozeman, Montana 59715

(Received 9 February 1972; revised manuscript received 24 May 1972)

Photoemission spectra are used to identify unusually narrow chemisorbed levels of O^{2-} on Ba and Sr at 4.6 and 4.8 eV below the Fermi level E_F, respectively. Nitrogen on Ba forms narrow states 1.3 and 5.3 eV below E_F. Measurements of sticking probability and of electron emission in the dark show that the oxygen-metal chemical activity is initially small, increases to a maximum, and then abruptly decreases as the mass of oxide increases.

Detailed knowledge of the interaction of a gas and a solid surface is important to both science and technology. Reported in this communication are the first direct and detailed observations of a gas-solid interaction with ultraviolet photoemission spectroscopy (UPS) combined with measurements for the mass of sorbed gas and "chememission" (electron emission in the dark during gas exposure). In addition to obtaining the electronic structure at various states of reaction, we obtained information about the reaction kinetics. The systems observed were Ba and Sr exposed to O_2 as well as the exposure of Ba to N_2 and H_2. The oxide systems were studied from submonolayer oxide coverages to oxides thick enough to obtain bulk-oxide UPS data. The chemisorbed oxygen and nitrogen from very narrow atomiclike states on Ba and Sr, in contrast to the broad states formed by oxygen on Ni, Ti, Tl, and Pb.[1,2] It is also found that the chemisorbed oxygen on Ba and Sr enhances the photoemission from the metal. The observations indicate that the thin oxide forms a crevicelike structure rather than a uniform film.

An *in situ* two-step evaporation technique was used for sample preparation making possible maximum pressures *during* sample deposition of $(2-8)\times 10^{-10}$ Torr. The second step used a Mo ribbon evaporator which was well "outgassed" prior to receiving a charge from the primary

evaporator. About 50 cm from the Mo ribbon two side-by-side samples were prepared, one on the photocathode and the other on the quartz crystal of the oscillator microbalance which had a stability of ± 0.1 Hz/hr. Thus the mass change of the microbalance sample mimicked the photocathode sample, with a sensitivity equivalent to 0.1×10^{14} O atoms cm^{-2}. The leak-valve and ion-pump ports had no line-of-sight path to the samples or the nude ion gauge that was placed very near the samples. The instrumentation used to obtain the UPS data has been reported previously.[3]

Direct information about the resultant products of the gas-metal reaction is obtained by examining the UPS properties of the composite sample before and after a gas exposure. Shown in Fig. 1 are the energy-distribution curves (EDC's) obtained at the photon energy $h\nu = 11.2$ eV. The curves are plotted versus the initial state energy E; the Fermi energy E_F is chosen to be zero. Figure 1(a) shows an EDC for unexposed Ba. The

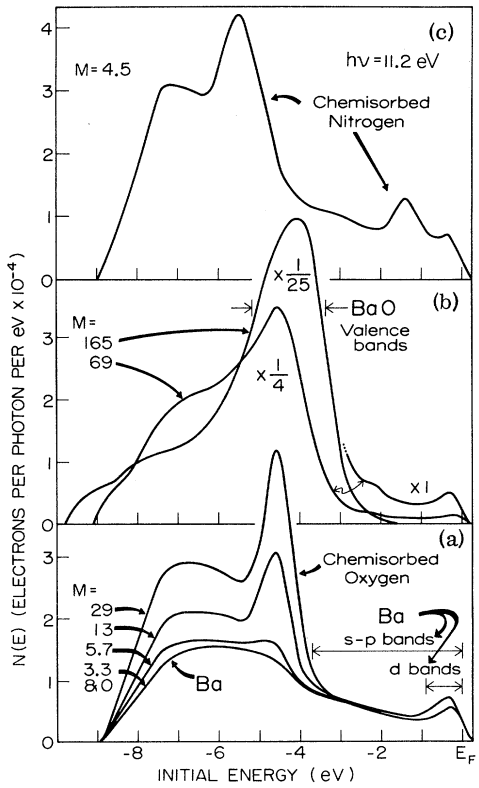

FIG. 1. Photoemission EDC's at $h\nu = 11.2$ eV from Ba, Ba exposed to O_2 and N_2, and BaO, all plotted as functions of initial energy. The mass of sorbed gas, M, in units of 10^{14} atoms cm^{-2} are noted for each EDC. The EDC's in (b) have been reduced in size.

peak just below E_F, with an 0.8-eV width, is emission from Ba d bands. A slight inflection, which is not discernible in the curve shown, occurs at -3.7 eV, and it is probably produced by the bottom of the s-p bands.[4] A large fraction of the electrons observed in the EDC are low-energy scattered electrons resulting from pair production. The results for subsequent O_2 exposures X are shown in Fig. 1(a) for small $X \lesssim 200$ L and Fig. 1(b) for large X.[5] The relative amplitudes of the EDC's are accurate to a few percent. The total O mass adsorbed, M, in units of 10^{14} atoms/cm^2, is noted for each curve.

The data in Fig. 1(a) show two effects. (1) For very small $X \lesssim 13$ L, a mass change $M \lesssim 3.3$ is observed, and no change is observed in the EDC's. This initial mass increase is apparently due to oxygen diffusion into the Ba film. (2) Additional exposures produce a strong, very narrow initial state centered at -4.6 eV. (See the EDC's for $M = 13$ and 29.) The $M = 13$ curve, for example, had an exposure of 97 L at 1×10^{-7} Torr. The work-function changes were less than 0.1 eV. The area of the "spike," considering it to be an additive effect, is proportional to O uptake. Much of the observed width of the spike is attributable to the resolution of the instrumentation.[6]

Since the narrow sorbate state develops on subsequent O_2 exposure into the valence bands of BaO, the state is identified as a bound state derived from the $2p$ shell of O^{2-}. The narrow width of the state is unusual for adsorbed species and indicates that it is atomiclike. In contrast, results obtained in our laboratory[1] on Pb and Tl as well as those reported[2] for Ni and Ti show a very wide adsorbate state for all levels of O_2 exposure.

Examination of the heavy-oxide data, which is exemplified by the $M = 165$ EDC in Fig. 1, shows it to be characteristic of BaO.[7] The large 2.75-eV-wide peak is due to the BaO valence bands (VB). As $h\nu$ changes, the shape of the VB peak changes; this is a manifestation of crystal-momentum–conserving transitions (direct model). The VB emission threshold of $\simeq 5$ eV is in good agreement with the accepted band gap and electron affinity of 4.4 and 0.6 eV, respectively.[8] Also note that (i) the fraction of scattered electrons is small because of the large threshold for inelastic scattering, and (ii) the probability for photoemission is much larger for the O atomiclike states than for the Ba free-electron–like metallic states.

Parallel experiments have been done on the ox-

idation of Sr. The results are very similar to those discussed above for Ba. The narrow O^{2-} sorbate states[9] are 4.8 eV below E_F and the width of the SrO VB is 2.0 eV.

Barium sorption studies with N_2 and H_2 were also made; however, H_2 exposure produced no detectable effects. Figure 1(c) shows the effects of N_2 exposure. In order to obtain a reaction, the Ba was exposed to 2×10^{-4} Torr for ~5 min. Two atomiclike sorbate states at −1.3 and −5.5 eV formed at a coverage of 4.5×10^{14} N atoms/cm^2.[10] Doubling the N_2 exposure produced no further effects. Since the energies of these states are very much smaller than the ionization energy[11] of 15.51 eV for N_2 and 14.53 eV for N, it is not likely that they result from chemically shifted states of an N or N_2 sorbate. In analogy with the oxygen results, a possible explanation for the −5.5-eV peak is a state derived from the $2p$ orbitals of N. Note that the p orbitals of O were shifted by 9 eV when filled by the ionic transfer and placed in the electronic environment of the oxide sorbate structure (the ionization energy for O is 13.61 eV[11]). A shift of 9.0 eV is also obtained if the nitrogen sorbate level is due to a nitrogen ion with an electronic structure similar to a closed electronic shell. Within this scheme the relative energies and amplitude of the peaks suggest that the −1.3-eV peak is due to a state derived from a Ba orbital.

Contrary to the expected behavior for a uniform-layer model for the sorbate, the metallic component (the alkaline-earth d state) of the emission is not attenuated by smaller amounts of chemisorbed O or N ions. In fact two counter characteristics are noted. (A) For the smaller $h\nu$'s the observed amplitudes of the peak resulting from metallic d emission are enhanced after the initial O_2 exposures, and only for the larger $h\nu$'s is a slight attenuation observed (see Fig. 1). (B) The metallic emission persists for rather large sorbate coverages. These characteristics are displayed in Fig. 2(a) where the ratios of the d-peak amplitudes with respect to the fresh metal for the $h\nu=7.7$-eV EDC's are plotted as a function of M. Further, as seen in Fig. 1, another enhancement is observed for the number of slow electrons. The latter enhancement is probably not due to an increased number of scattered electrons since there is no corresponding decrease of primaries. The strength of the enhancement in both cases is largest near threshold and decreases as the final-state energy increases. The data allow the view that both enhancements

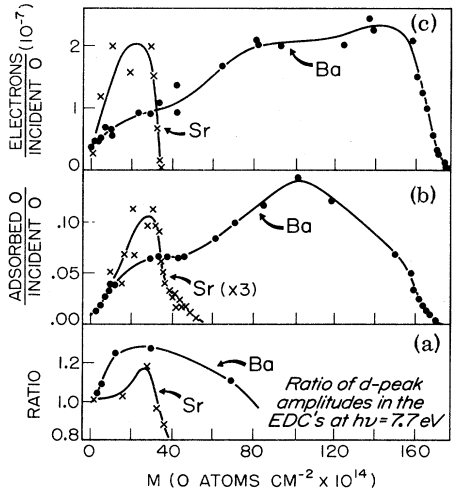

FIG. 2. (a) The metallic emission enhancement, (b) an apparent sticking coefficient, and (c) the chememission yield, all plotted as functions of the sorbed oxygen mass on Ba and Sr.

may result from the same phenomenon.

The persistence of the metallic emission can be accounted for by the model proposed below for the oxidation kinetics. For a possible explanation of the adsorbate-enhanced metallic emission we suggest that the optical coupling is increased by a small admixture of the atomiclike sorbate wave function. The suggestion is based on the typical property that optical coupling for atomiclike wave functions is much larger than the coupling for free-electron–like wave functions.

The kinetic properties for the oxidation of Ba and Sr are exemplified by two sets of data obtained in these experiments. The first is the ratio of the number of atoms adsorbed to those incident on the surface, an apparent sticking coefficient. These coefficients are plotted versus M in Fig. 2(b). Pressure measurements and kinetic theory determine the number of incident atoms. The second, which is shown in Fig. 2(c), is the chememission per incident O (a chememission yield). The common characteristics of the data displayed in Figs. 2(b) and 2(c) show that the reactivity of the solid-gas interface begins at a small value, increases for initial oxidations, and then within the activity regime of the experiments has an abrupt cutoff.

These reaction phenomena may be understood by recalling the persistence of the metallic d emission in the EDC's for M's less than the cutoff, and by noting that the metal-metal distance is much shorter in the oxides than in the metal. It is possible to account for all of the observations

with a model which requires a large number of crevices in the oxide layer. The apparent increase in reactivity would then result from (I) exposure of unreacted Ba produced by surface "tearing" to accomodate the shorter metal-metal distance and from (II) mechanical trapping of the incident oxygen in the crevice structures. The word apparent is used here as well as above in connection with the sticking coefficient since multiple oxygen collision within the crevice structures during the trapping could account for the observations without requiring an increase in the reaction probability per collision.[12] In addition to oxygen moving in the crevices towards the metal substrate, metal atoms may migrate on crevice surfaces toward the vacuum. The net reaction is cut off when the oxide's growth forms an oxide layer which no longer contains direct openings between the vacuum and the metal.

Photoemission observations, in addition to those displayed in Fig. 1, support a contiguous-layer model for oxide thickness greater than the cutoff. That is, for sufficiently small values of $h\nu$ the emission is from the metal substrate after transport through the oxide. Then, as $h\nu$ increases, the metallic substrate emission is attenuated by hot-electron inelastic scattering in the oxide and by optical absorption in the oxide.[7]

The data in Figs. 2(b) and 2(c) show that the level of activity and the cutoff mass are smaller for Sr than for Ba. Yet the oxide heat of formation per molecule is 5.8 and 5.5 eV for Sr and Ba, respectively. Also the increased number of metallic atoms per unit volume in the oxide is 1.6 and 1.5 for Sr and Ba, respectively.[11] The available energies and increased density factors do not account for the differences in the oxidation of Ba and Sr. We suggest that the difference is a result of the crystal structure changes in the Ba case (Ba is body centered cubic while Sr and the oxides are face centered cubic).

The sorbate states observed in these experiments have unusually narrow widths. The states could be related to the type obtained in Newns's calculations for a hydrogenic adsorbate.[13] The calculations show that narrow, bound states may form just below the substrate bands. All the states observed here are below the bands if one considers the shallow nitrogen sorbate state to be below the *d* bands. Another possible explanation for the width is adsorbate isolation, in either the adsorbate-adsorbate or adsorbate-substrate distance. Calculations by Gadzuk, Hartman, and Rhodin indicate that narrow states can exist for very modest adsorbate-substrate distances.[14] The existence of some sorbates' isolation is not necessarily inconsistent with the proposed oxide-crevice-growth model since the crevices increase the "surface area" and correspondingly increase the opportunities for a one- or a two-dimensional bonding geometry.

We wish to thank E. B. Hensley, N. V. Smith, and E. W. Plummer for helpful discussions. We are particularly indebted to our colleagues J. Hermanson and P. Callis for many illuminating discussions and suggestions.

---

†Research sponsored by the U. S. Air Force Office of Scientific Research, Office of Aerospace Research, under Contract/Grant Nos. AF-AFOSR-68-1450 and AF-AFOSR-71-2061.

*Present address: 5509 Holmes Run Parkway, Alexandria, Va. 22304.

[1]G. J. Lapeyre, A. D. Baer, and K. A. Kress, to be published.

[2]D. E. Eastman and J. K. Cashion, Phys. Rev. Lett. 27, 1520 (1971).

[3]K. A. Kress and G. J. Lapeyre, Rev. Sci. Instrum. 40, 74 (1969).

[4]K. A. Kress and G. J. Lapeyre, to be published. Detailed studies of the curvature of the EDC's were made by also measuring the second derivation of the EDC's.

[5]1 L $\equiv 1\times10^{-6}$ Torr sec, a Langmuir.

[6]The resolution can be estimated from the shape of the emission coming from the region near E_F. Ideally it would be nearly a step function; however, the observed Fermi edge width is ~0.3 eV.

[7]G. J. Lapeyre and K. A. Kress, to be published.

[8]C. Y. Hu and E. B. Hensley, J. Appl. Phys. 40, 3346 (1969).

[9]C. R. Helms and W. E. Spicer, Phys. Rev. Lett. 28, 565 (1972), reported the observation of a narrow oxide peak on Sr and the persistence of the metallic emission.

[10]Studies of this kind should be complemented by other analytical tools (e.g., Auger spectroscopy and residual gas analysis) so trace contaminants may be unequivocally ruled out. Measurements above the LiF cutoff (11.8 eV) would also be valuable.

[11]*Handbook of Chemistry and Physics* (The Chemical Rubber Co., Cleveland, Ohio, 1968), 49th ed.

[12]The ability of a film to trap oxygen is supported by the observation that samples lost mass if the oxidation procedure was interrupted. The loss (a few percent of the mass increase) was observed after the samples sat in vacuum a few hours. The changes in the EDC's that accompanied the mass loss were consistent with O loss from the sample. In addition it was found that a film which had some oxide on it and which had been in vacuum for a while would show (for a few minutes) a sticking coefficient that was larger than that of Fig.

2(b). The experiments were not extended to obtain the data needed for a detailed description of these hysteresislike properties of the oxidation processes.

[13]D. M. Newns, Phys. Rev. 178, 1123 (1969).
[14]J. W. Gadzuk, J. K. Hartman, and T. N. Rhodin, Phys. Rev. B 4, 241 (1971).

Screening of Wannier Exciton States near the Metal-Insulator Transition

Baruch Raz, Aharon Gedanken, Uzi Even, and Joshua Jortner
Department of Chemistry, Tel-Aviv University, Tel-Aviv, Israel
(Received 4 April 1972)

We provide a new spectroscopic criterion for the observation of the insulator-metal transition in a two-component system, which is based on the disappearance of Wannier exciton states in the metallic region. This effect has been observed in the vacuum-ultraviolet spectra of mercury/xenon mixtures deposited at 10–30°K, where the Xe Wannier states are abruptly washed out at (55 ± 5)% of Hg.

Metal-nonmetal transitions in ordered and disordered systems[1] have been experimentally induced by structural modifications,[2] by the application of external fields,[3] by concentration changes in two-component systems,[4-6] and by density changes in a one-component system.[7,8] Most of these studies[1] monitored the electrical transport properties and the magnetic properties of the system undergoing the MNM transition. We advance a new spectroscopic criterion for the observation of the MNM transition. Wannier-Mott excitons in a two-component system, consisting of open-shell metallic atoms and of closed-shell saturated atoms, are utilized as a spectroscopic probe to monitor the MNM transitions. These large-radius excited states are expected to persist only in the insulating state, and become unbound in the metallic state because of short-range dielectric screening effects.

Our experimental approach is based on Mott's argument concerning the effects of long-range forces on the MNM transition.[9] The long-range electron-hole potential in the nonmetallic state,

$$V(r) = -e^2/\mathcal{K}r \tag{1}$$

(where $\mathcal{K}$ is the static dielectric constant), is replaced in the metallic state by a short-range potential, which according to the Thomas-Fermi prescription is

$$V(r) = -(e^2/\mathcal{K}r)\exp(-qr), \tag{2}$$

where the screening length is

$$q^2 = 4m^*e^2(3n/\pi)^{1/3}/\hbar^2\mathcal{K}, \tag{3}$$

with n corresponding to the free-electron density. As it is well known,[9] the potential well (2) does not have bound states for

$$qa_H > 1.0, \tag{4}$$

where the modified Bohr radius[9] is $a_H = \hbar^2\mathcal{K}/m^*e^2$, while m^* represents the electron effective mass.

Consider the implications of these arguments for the description of Wannier-Mott–type shallow and deep exciton and impurity states.[10,11] In a nonmetallic solid[10] the Coulomb electron-hole attraction is dielectrically screened, whereupon for large-radius states the microscopic variation of the crystal and of the positive-hole potentials is replaced by Eq. (1). Furthermore, when the conduction band is wide and parabolic, the effects of the crystal potential can be subsummed into an effective mass.[10,11] The envelope function for large-radius exciton and impurity states obeys the equation

$$[-(\hbar^2/2m^*)\nabla^2 + V(r) - E]\psi = 0, \tag{5}$$

where the potential is given by Eq. (1). A Rydberg series converging to the bottom of the conduction band has been experimentally observed for shallow states in semiconductors[12] and for deep-lying states in rare-gas solids.[13] The observation of exciton states in dense rare gases is independent of symmetry arguments, and these excited states are amenable to experimental observation in positionally disordered systems (i.e., liquid rare gases)[14] and in substitutionally disordered systems (i.e., heavily substituted rare-gas alloys).[15] Now, when an insulator (such as a rare-gas solid) is gradually substituted by unsaturated metal atoms, this two-component system may eventually undergo a MNM transition, whereupon $V(r)$ in Eq. (5) will take the ap-